Baltic Astronomy, vol. 15, 207–210, 2006.

HELIUM, CARBON AND SILICON ABUNDANCES IN THE HW VIRGINIS ECLIPSING BINARY SUBDWARF-B PRIMARY

A. N. Mortimore and A. E. Lynas-Gray

Department of Physics, University of Oxford, Denys Wilkinson Building, Keble Road, Oxford OX1 3RH, U.K.

Received 2005 August 15

Abstract. Light curve solutions show HW Vir and PG 1336-018 to be remarkably similar eclipsing binaries. The subdwarf-B (sdB) primary of PG 1336-018 is a pulsator but pulsation is not detected in the sdB primary of HW Vir. Ultraviolet spectra were used to obtain carbon and silicon abundances in the sdB primary of HW Vir; in due course these should be compared with those in the sdB primary of PG 1336-018 to see if pulsation in the latter could be explained by the κ-mechanism, arising from higher metal abundances and microscopic diffusion.

Key words: stars: hot subdwarfs – stars: abundances – stars: individual (HW Vir)

1. INTRODUCTION

HW Vir (BD –07 3477) is reported by Menzies & Marang (1986) to be an eclipsing binary with an orbital period of 0.1161 days, the primary being a sdB star. Much subsequent work is concerned with an interpretation of the period change, first identified as a decrease by Kilkenny et al. (1994). İbanoğlu et al. (2004) find a sinusoidal variation in residuals between observed and calculated times of mid-eclipse which they suggest is due to a third body in the system; a brown dwarf orbiting with a period of 18.8 years, and having a mass between 0.022 $M_{\odot}$ and 0.07 $M_{\odot}$ depending on the inclination of its orbit.

Kilkenny et al. (1998) discover NY Vir (PG 1336-018) to also be an eclipsing binary with a remarkable resemblance to HW Vir; the essential difference is the pulsation in the sdB primary of PG 1336-018, and the non-detection of change in the binary orbital period (Kilkenny 2005). The similarity between HW Vir and PG 1336-018 is indicative of the absence of a clear separation between pulsating and non-pulsating sdB stars in the $T_{\rm eff}$ vs. $\log g$ diagram (Koen et al. 1999). Charpinet (2001) reviews earlier theoretical work which explains sdB star pulsation as being driven by a metal ionization zone, its required overabundance of metals being provided by microscopic diffusion from outer layers.

A comparison of photospheric abundances in HW Vir and PG 1336-018 could serve as a verification of our understanding of sdB star pulsation. As a first step, metal abundances were determined for HW Vir from International Ultraviolet

Explorer (IUE) spectra. Different $T_{\rm eff}$ and $\log g$ values are obtained from light curve solutions (Kiss et al. 2000) and Balmer line fits (Wood & Saffer 1999), prompting a new determination with ultraviolet spectroscopy.

2. OBSERVATIONS

HW Vir was observed with IUE on 1984 May 10 and 11. On May 10 a series of low dispersion spectra were obtained using the Long Wavelength Prime (LWP) camera. While reading the LWP camera, a high dispersion spectrum was accumulated in the Short Wavelength Prime (SWP) camera and only read once an adequate exposure had been achieved. During May 11 the role of the two cameras was reversed, leading to a series of low dispersion SWP spectra and accumulation of LWP high dispersion spectra while reading the SWP camera. Images were reprocessed (Nichols & Linsky 1996) and spectra extracted.

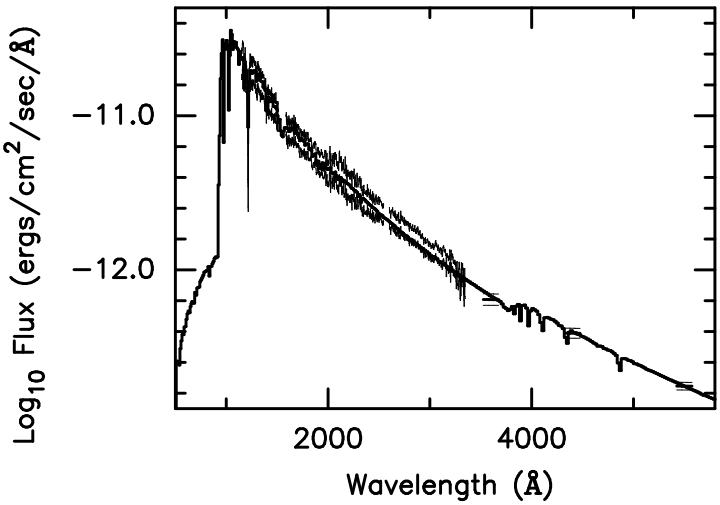

Fig. 1. The energy distribution of HW Vir.

3. EFFECTIVE TEMPERATURE AND ANGULAR RADIUS

The energy distribution of HW Vir is based on IUE images SWP 22985, SWP 22986, LWP 03322 and LWP 03323; these are supplemented by fluxes in U, B and V passbands derived from photometry by Menzies et al. (1990). SWP 22984 was obtained during primary eclipse and not therefore included. Other low resolution SWP and LWP spectra obtained at various orbital phases give flux densities which agree within error limits, indicating the absence of an ultraviolet reflection effect. Remie & Lamers (1982) iteration was used for $T_{\rm eff}$ determination with trial reddening estimates in the range $0.00 \leq E_{B-V} \leq 0.04$, calculated following Seaton (1979), which attempt to remove the 2200 Å feature.

Thin lines in Figure 1 are dereddened UBV flux densities and merged IUE low resolution spectra for $E_{B-V} = 0.00$ and $E_{B-V} = 0.04$. UBV flux densities for $E_{B-V} = 0.02$ are similarly shown as thick lines. The remaining thick line in Figure 1 is the flux density at the top of the Earth's atmosphere estimated

from the adopted model stellar atmosphere, computed following Kurucz (1992), normalized at V for $E_{B-V} = 0.02$. Reddening along the line of sight to HW Vir is therefore $E_{B-V} = 0.02 \pm 0.02$ and $T_{\rm eff} = 29\,400 \pm 700$ K with a corresponding angular radius $\alpha = (2.03 \pm 0.06) \times 10^{-11}$ radians. Upper and lower $T_{\rm eff}$ and α limits correspond to the uncertainty in E_{B-V}.

4. SURFACE GRAVITY AND ABUNDANCES

High dispersion spectra from images SWP 22971, SWP 22972 and SWP 22973 were corrected for relative velocity shifts and merged. Abundances and surface gravity were determined by comparison with synthetic spectra computed with SYNSPEC (Hubeny & Lanz 2003) assuming local thermodynamic equilibrium (LTE), using model stellar atmospheres computed with ATLAS9 (Kurucz 1992). The version of SYNSPEC used differed from the public domain version in that He I line Stark broadening was computed using tables by Dimitrijević & Sahal-Bréchot (1984, 1990) as appropriate. Synthetic spectra were broadened to allow for orbital motion and rotation of the sdB, assuming the binary is tidally locked.

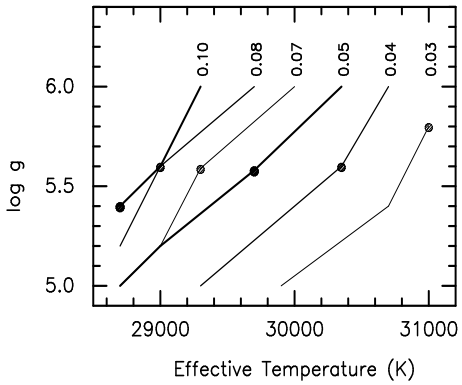

Fig. 2. Loci of fits to He II at 1640 Å.

Table 1. Carbon and silicon abundances.

$T_{\rm eff}$ (K)	log g	Si IV λ (Å) 1394 1403	Si III λ (Å) 1299	C IV λ (Å) 1548 1551	C III λ (Å) 1247
28700	*5.0*	*0.06*	*0.21*	*0.008*	*0.030*
	5.6	*0.07*	*0.16*	*0.014*	*0.030*
	6.0	*0.08*	*0.13*	*0.023*	*0.030*
29350	*5.0*	*0.06*	*0.28*	*0.006*	*0.027*
	5.6	*0.07*	*0.21*	*0.011*	*0.030*
	6.0	*0.08*	*0.16*	*0.017*	*0.032*
30100	*5.0*	*0.06*	*0.39*	*0.005*	*0.029*
	5.6	*0.07*	*0.29*	*0.008*	*0.030*
	6.0	*0.08*	*0.21*	*0.033*	*0.033*

Determination of surface gravity and helium abundance was based on the He II 1640 Å line. Loci of fits in the $T_{\rm eff}$ vs. $\log g$ diagram are shown in Figure 2 as lines of differing thickness annotated by helium abundances (by number) relative to the Sun. Large filled circles show the best fit obtained for each helium abundance.

Allowing for error limits on the derived $T_{\rm eff}$, Figure 2 shows the helium abundance (by numbers) to lie between 0.04 and 0.10 of the solar helium abundance and $\log g$ to lie between 5.4 and 5.8. The derived helium abundance by numbers for sdB primary of HW Vir was therefore $n({\rm He}) = 0.07 \pm 0.03$ of the solar value; its surface gravity was similarly, $\log g = 5.6 \pm 0.2$.

Few metal lines were readily identified in high dispersion spectra though lines of Si III, Si IV, C III and C IV could be used for abundance determinations by direct comparison with synthetic spectra. Abundances by number, relative to the Sun, obtained for several assumed $T_{\rm eff}$ and $\log g$ values are presented in Table 1. Abundances obtained appear to be ionization stage dependent; synthetic spectrum calculations in non-LTE do not explain the apparent discrepancies.

In the case of carbon, abundances from C III and C IV lines do not appear to

be significantly different in view of uncertainties in $T_{\rm eff}$ and $\log g$ and weakness of the C IV, all are formed at similar depths in the atmosphere. Silicon abundances are better determined because the lines are stronger and the difference between Si IV and Si III appears to be real; this could arise because of stratification in the atmosphere because the Si IV and Si III lines are formed at Rosseland mean depths of 4×10^{-7} and 10^{-3}, respectively.

5. CONCLUSIONS

The $T_{\rm eff}$ lower limit is just above the Wood & Saffer (1999) upper limit but the derived helium abundance and surface gravity were in good agreement. Both silicon and carbon are depleted relative to the Sun. The difference between silicon abundances derived from Si IV and Si III lines suggests a stratified atmosphere caused by microscopic diffusion, though further work on abundance gradients would be needed for confirmation.

Hipparcos parallax measurements indicate, at 68 % confidence, a distance to HW Vir of not less than 264 pc. The angular radius lower limit derived in this paper then suggests a HW Vir sdB primary radius of not less than 0.22 $R_\odot$. Light curve solutions (see Kiss et al. 2000) indicate 0.22 $R_\odot$ as an upper limit for the radius of the sdB primary, which suggests a discrepancy unless $E_{B-V} = 0.0$ in which case $T_{\rm eff}$ is close to the lower limit suggested by the ultraviolet energy distribution and in agreement with Wood & Saffer's (1999) result.

REFERENCES

Charpinet S. 2001, Astron. Nachr., 322, 387

Dimitrijević M. S., Sahal-Bréchot S. 1984, JQRST, 31, 301

Dimitrijević M. S., Sahal-Bréchot S. 1990, A&AS, 82, 519

Hubeny I., Lanz T. 2003, http://tlusty.gsfc.nasa.gov/Synspec43/synspec.html

İbanoğlu C., Çakirl Ö., Taş G., Evren S. 2004, A&A, 414, 1043

Kilkenny D. 2005, private communication

Kilkenny D., Marang F., Menzies J. W. 1994, MNRAS, 267, 535

Kilkenny D., O'Donoghue D., Koen C., Lynas-Gray A. E., Van Wyk F. 1998, MNRAS, 296, 329

Kiss L. L., Csák B., Szatmáry K., Fũrész G., Sziládi K. 2000, A&A, 364, 199

Koen C., O'Donoghue D., Kilkenny D., Stobie R. S., Saffer R. A., 1999, MNRAS, 306, 213

Kurucz R. L. 1992, in *The Stellar Populations of Galaxies*, IAU Symp. 149, eds. B. Barbuy & A. Renzini, Reidel Publ. Company, Dordrecht, p. 225

Menzies J. W., Marang F. 1986, in *Instrument and Research Programmes for Small Telescopes*, IAU Symp. 118, eds. J. B. Hearnshaw & P. L. Cottrell, Reidel Publ. Company, Dordrecht, p. 305

Menzies J. W., Marang F., Westerhuys J. E. 1990, SAAO Circ. 14, 1

Nichols J. S., Linsky J. L. 1996, AJ, 111, 517

Remie H., Lamers H. J. G. L. M. 1982, A&A, 105, 85

Seaton M. J. 1979, MNRAS, 187, 73p

Wood J. H., Saffer R. 1999, MNRAS, 305, 820